Small-scale variability of soil properties and soil-vegetation relationships in patterned ground on different lithologies (NW Italian Alps).

Michele D'Amico[1a], Roberta Gorra[1], Michele Freppaz[1]

[1]Università degli Studi di Torino, DISAFA. Largo Braccini 2, 10095, Grugliasco (To), Italy

[a]Corresponding author: ecomike77@gmail.com

Abstract

Cryogenic patterned ground represents spectacular periglacial landscapes. On the Alps, sorted/nonsorted patterned ground features larger than 1 m, formed by deep seasonal cryoturbation with or without permafrost, occupy exposed, stable surfaces at high altitudes and represent a particularly harsh habitat for plant life.

We analyzed soils across transects through typical active patterned ground features (sorted/nonsorted circles and stripes) on four common lithotypes (calcschists, serpentinite, gabbros and gneiss) in the Western Italian Alps, in order to observe the small-scale lateral and depth variability in physico-chemical properties, and their association with cryoturbation, plant cover and species distribution.

Cryoturbation was correlated with lateral/vertical textural sorting across features, mostly visible on silt and coarse sand, but with opposite trends on sorted and nonsorted patterned ground types. A strong lateral variability in organic carbon was detected, with high values near the better vegetated rims and low contents in the centers. Exchangeable bases, heavy metals and nutrients followed the same distribution. However, the differences inherited from the parent materials were overwhelming.

Climate is the main driver of high altitude ecosystems, reducing total plant cover and causing cryoturbation, which in turn creates strong edaphic gradients over small distances. Plant species and communities are well correlated with edaphic properties inherited from the parent materials, such as exchangeable Ca and heavy metals.

Highlights

- parent material weatherability influenced patterned ground type;
- patterned ground type associated with different textural sorting;
- parent material/cryoturbation correlated with small-scale chemical differentiation;
- plant cover correlated with altitude and climate;
- soil chemistry associated with plant species distribution.

Keywords

Cryoturbation; pedogenesis; periglacial soils; serpentine soils; sorted patterned ground; nonsorted patterned ground

1 Introduction

Patterned ground develops as a result of cryoturbation, which consists in the mixing, heaving, churning of soils associated with differential displacement of particles with different dimensions, thaw consolidation and and/or other phenomena associated with density variations, occurring during freeze-thaw cycles (Washburn, 1980; Bockheim and Tarnocai, 1998; Ballantyne, 2013). It is common in Arctic and subarctic regions (e.g., Etzelmüller and Sollid, 1191), where sorted nets, stripes and nonsorted mud boils and hummocks characterize large surfaces and are the most spectacular features of cold desert and tundra landscapes. Frost-sorted patterned ground is defined by the segregation of stony sections separating cells or stripes of relatively clast-free soil (Ballantyne, 1996), while nonsorted patterned ground includes well vegetated earth hummocks or nonsorted circles/stripes and mud boils, where bare soil is surrounded by a more developed vegetation belt. With the exception of hummocks, active patterns are recognizable as their inner part is covered by bare or sparsely vegetated soil, by the absence of lichens on stones and other indicators.

The spatial arrangement of fine particles and clasts, and of vegetated and bare surfaces, creates a strong small-scale variability in the distribution of soil properties and plants (Ugolini, 1966; Anderson and Bliss, 1998; Ugolini et al., 2006). The depth, speed and intensity of cryoturbation processes and the consequent disturbance within patterned ground features varies depending on microsite location, thus partitioning the plant habitat into repeated spatial units (Johnson and Billings, 1962). The central parts experiences longer and more intense periods of frost disturbances than the rims, both during daily, superficial freeze-thaw cycles, and during deeper seasonal frost heave; the rims, in turn, are subjected only to shallower seasonal cycles (Ballantyne, 2013). This different sensitivity to frost churning and surface settling significantly influences small-scale physical gradients, which have strong impacts on the survivorship and reproduction of vascular plants and on community composition (Jonasson and Sköld, 1983; Jonasson, 1986; Anderson and Bliss, 1998; Haugland, 2004; Cannone et al., 2004; Haugland and Owen, 2005). In turn, high vegetation cover on the borders reduces the movement associated with frost disturbances (e.g., Walker et al., 2004). The spatial distribution of plant cover influences organic matter turnover, accumulation and nutrient cycling in soils: available soil nutrients, organic carbon (TOC) and exchangeable bases are normally higher close to the rims, while pH is higher in the center, where the cation exchange capacity is lower because of low TOC and because of fresh, weakly weathered materials upwelled to the surface during convective movements associated with differential frost heave (e.g., Michaelson et al., 2012; Walker et al., 2004).

Contrarily to its importance in high latitude landscapes, patterned ground is quite rare in high-altitude, mid-latitude mountain ranges, mostly because of steep slopes and strong erosive processes; they are thus generally restricted to few flat or gently sloping surfaces, particularly in positions exposed to snow removal by wind during winter months (Johnson and Billings, 1962): deep snow cover, in fact, reduces the depth and intensity of soil freezing and cryoturbation during winter, limiting the cryogenic processes (zero-curtain effect). At the same time, abundant

77 water availability is necessary, consequently concave morphologies are often associated with
78 well-developed patterned ground morphologies (Feuillet, 2011). Few examples of patterned
79 ground habitats have been studied in mid-latitudes mountain ranges (e.g., Johnson and Billings,
80 1962; Beguin et al., 2006; Feuillet, 2011; Gerdol and Smiraglia, 1990; Matsuoka et al. 2003;
81 Munroe, 2007), but only seldom chemical soil properties were analyzed. These large patterned
82 ground features in mid-latitude mountain ranges are often relicts of colder periods (e.g., Munroe,
83 2007); if active, they are mainly caused by seasonal freeze-thaw cycles, and are usually
84 associated with the presence of permafrost (Goldthwait, 1976). In fact, active cryoturbation has
85 been described only in few cases in mid-latitude mountain ranges, also in presence of
86 permafrost: the thick active layer reduces the possibility of ice lensing and the volume change
87 responsible for the effective development of cryoturbation features (Bockheim and Munroe,
88 2014). On the Alps, active patterned ground is often characterized by small features, derived
89 from daily freeze-thaw cycles (e.g., Matsuoka et al., 2003).
90 Active patterned ground is vulnerable to climate change. A reduced activity in cryoturbation
91 processes has already been observed (e.g., Gerdol and Smiraglia, 1990), and resulted in an
92 expansion of plant cover and the progression of vegetation succession from pioneer species
93 towards more acidophilous grassland ones.
94 The parent material lithology is important in the formation and development of different
95 patterned ground features (Matsuoka et al., 2003) and, thanks to different resistance to physical
96 weathering, leads to sorted or nonsorted features (the latter associated with easily weatherable
97 materials). The parent material lithology should also have strong effects on soil chemical
98 properties which are heavily impacted by cryoturbation and, in turn, have a strong effect on plant
99 colonization. However, small scale variability of soil chemical properties associated with
100 cryoturbation and its relationships with vegetation are seldom studied, and only few works deal
101 with the mutual effects of soil chemistry, cryoturbation and vegetation patterns (e.g., Cannone et
102 al., 2004; Jonasson and Sköld; 1983; Michaelson et al., 2012).

Given the high vulnerability of high altitude plant communities under a changing climate (Körner, 2003), the investigation on how different substrate lithologies affect the soil properties contributing to plant distribution in a high elevation landscape, characterized by patterned ground phenomena, is fundamental. We thus chose four patterned ground landscapes with different parent materials in an understudied Western Alpine area characterized by the presence of large sorted or non-sorted features. Our hypothesis was that cryoturbation and patterned ground development should enhance the edaphic differences associated with parent material lithology, and should create strong edaphic gradients able to influence plant ecology. This study was thus configured to: a) investigate the morphology and characteristics of soils associated with well-developed, active patterned ground in an understudied, mid-latitude, high altitude alpine habitat; b) to evaluate the contribution of the edaphic properties inherited from the parent material lithology, their redistribution caused by patterned ground activity and cryoturbation, to the vegetation cover and species distribution.

2 Materials and Methods

2.1 Study area

Sorted and nonsorted patterned ground landscapes occupy only small favorable surfaces but are quite widespread in the Western Italian Alps. We chose four active large patterned ground areas on common lithotypes in the Graian Alps in north-western Italy, in Piemonte and in Valle d'Aosta regions.

Flat sampling sites were dominated by sorted or nonsorted circles, while gentle slopes by large sorted stripes (Table 1). On slopes steeper than 7°-10°, patterned ground was not observed. The parent materials were till composed of calcschists (Champorcher Valley, CS site), serpentinite and metamorphic gabbros in Champdepraz Valley (respectively, SP and GB sites), and frost shattered bedrock composed of gneiss (Piata Lazin, Val Soana, GN site). In CS and GB, the

128 calcschist and gabbroic parent materials were enriched in small quantities of serpentinite derived
129 from upslope areas. Sites CS, SP and GB were located in Mont Avic Natural Park, Aosta Valley,
130 while site GN was inside Gran Paradiso National Park, Piemonte (Figure 1). The mineralogical
131 composition of the studied lithologies was dominated by micas, calcite, quartz and smaller
132 amounts of feldspars/plagioclases (CS site), antigorite with small chlorite inclusions (SP site),
133 quartz, feldspars and micas (GN site), amphiboles (particularly actinolite and tremolite),
134 plagioclases, chlorites and traces of quartz (GB site). The presence of moraines and roches
135 moutonnées show that most study sites were under Pleistocene and Late Glacial ice sheets;
136 however, the morphology of Piata Lazin (GN site) resembles a relict peneplane remnant,
137 surrounded by steep glacier-eroded cliffs and glacial cirques, and does not bear any sign of past
138 glaciations. Abundant soil water is provided by a slightly concave topography (GN and GB sites)
139 and by streams derived from nearby rock glaciers (CS and SP sites). The thickness of the loose
140 material in which soils have developed is unknown.
141 The MAAT of the sampling sites is presumably between -5°C in GN site and ca. -3°C in the
142 others, and by MAP (rain and snow water equivalent) between ca. 1700 mm/y in GN and CS
143 sites (Mercalli and Cat Berro, 2005), and 1200-1300 mm/y in SP and GB sites (Mercalli, 2003).
144 Mean precipitation data were measured in weather stations located in nearby villages at lower
145 altitude, so higher values are expected in the sampling sites. No wind data is available for the
146 observed locations, but the exposed morphology is probably associated with strong winds and,
147 consequently, snow removal during winter. A high probability of permafrost is indicated by the
148 activity of patterns in excess of 2 m of diameter (Goldthwait, 1976), and other widespread
149 indicators, such as active rock glaciers, which are common on nearby slopes in every site, also at
150 a lower altitude. Moreover, according to the Alpine Permafrost Index Map (Boeckli et al., 2012),
151 the CS, GN and SP sites lye in the continuous alpine permafrost zone while GB lies in the area
152 where permafrost is likely found in cold conditions (Figure 1). However, the depth of the active

153 layer is unknown; at similar altitudes in the Alps, the active layer thickness is between 3 and 5 m
154 (Harris et al., 2009).
155 Soil temperature was measured at 10 cm depth from October 2007 to August 2008, using data
156 UTL-1 loggers in GN site. The mean soil temperature was equal to -1.7°C, whereas in late
157 winter, under a thick snow cover,(February-April) it was -3.9°C, with a minimum of -11.5°C
158 recorded on the 17th December 2007. The low temperature beneath a thick snow cover
159 confirmed the presence of permafrost (Imhof et al. 2000), despite the exceptionally warm air
160 temperatures observed during that winter at a regional scale. When the snowpack melted and the
161 water reached the ground, in May and June, the soil temperature remained stable at 0°C (zero
162 curtain effect), whereas after the complete melting the soil temperature fluctuated around 0°C
163 (summer months).
164 Soil sampling in all sites took place in late September 2012, when nighttime temperatures
165 normally drop below freezing point and freeze-thaw cycles become important.
166

167 **2.2 Field sampling strategy**

168 In each sampling area, soil pits were placed to dissect one complete, typical soil pattern (sorted
169 or nonsorted rock circle or stripe) from north to south. In order to reduce our impact on such
170 fragile and rare ecosystems, we chose to study only one typical pattern representative for each
171 area, based on the observation of surface morphology and the vegetation growing on many
172 features (15-20 in every site). We tried to sample only "simple" patterns, i.e. patterns which were
173 not divided into smaller and less differentiated sub-patterns. The soils were described across the
174 whole transects: genetic horizons were identified and morphological properties described
175 following standard methods (FAO, 2006). One sample was collected from these genetic horizons
176 (i.e., if an A horizon with homogeneous morphology was developed with different thickness
177 across most of the pattern, we collected a mixed sample from the whole horizon distribution). In
178 addition, five surface samples were collected equally spaced across the transect: two from the

opposite north and south stony/vegetated rims (N and S samples respectively), one in the center (C samples), two half-way from the center to the north and south borders (NC and SC samples respectively), at a depth between 1 and 10 cm, in order to detect relationships between chemical properties and vegetation patterns.

In order to obtain data regarding the small-scale effect of soil properties and cryoturbation processes on vegetation across the patterned ground transects, plant species (presence-absence data) were recorded on homogeneous (ca. 30x30 cm) areas around the sampling points, and plant species were recognized according to Pignatti (1992). Surface rockiness and bare soil were also visually evaluated on the same surfaces.

2.3 Soil analysis

The soil samples were air dried, sieved to 2 mm and analyzed following the methods reported by Van Reeuwijk (2002). The pH was determined potentiometrically in water extracts (1:2.5 w/w). The TOC and total N concentrations were measured by dry combustion with an elemental analyzer (CE Instruments NA2100, Rodano, Italy). Exchangeable Ca, Mg and Ni (later on, Ca, Mg, Ni) were determined after exchange with NH_4-acetate at pH 7.0, and their concentrations were measured by Atomic Absorption Spectrophotometry (AAS, Perkin Elmer, Analyst 400, Waltham, MA, USA); K and Na concentrations were measured as well but are not shown, as they were always very low and did not show trends across the considered patterned ground features nor associated with parent material variations. Available P (P_{Olsen}) was determined by extraction with $NaHCO_3$.

In order to evaluate weathering trends across the micro-scale transects, clay minerals were detected in surface S, C and N samples, and the mineralogy of coarse sand was characterized in the same samples in order to obtain a more precise lithological characterization of the parent materials. The mineralogy of the sand fraction was evaluated (3-80° 2θ) on backfilled, randomly

204 oriented powder mounts. The Mg saturated clay fraction (< 2 µm) was separated by
205 sedimentation, flocculated with $MgCl_2$, washed until free of Cl^-, and freeze-dried. Scans were
206 made from 3 to 35 º2θ at a speed of 1 º2θ min^{-1}, on air dried (AD), ethylene glycol solvated
207 (EG), and heated (550°C) oriented mounts. The presence of hydroxyl-interlayered minerals (HIV
208 and/or HIS) was ascertained, and their thermo-stability assessed, by heating the samples to 110,
209 330 and 550°C.
210

211 **2.3 Numerical elaborations**

212 Vegetation and soil-vegetation relationships were statistically analyzed using R 3.0.1 software (R
213 Foundation for Statistical Software, Institute for Statistics and Mathematics, Vienna, Austria).
214 Significant differences in soil parameters between different lithologies were checked and displayed
215 as boxplots, using the *multcomp* R package (Hothorn et al., 2008).
216 Vegetation types were classified using Cluster Analysis (CA), average linkage agglomeration
217 criteria, Bray-Curtis dissimilarity algorithm. As the number of sites was rather small, the number of
218 clusters to be considered during the following analysis was mainly chosen according to their
219 ecological significance.
220 Vegetation gradients within the different patterned ground sites and subsites were observed using
221 unconstrained ordination methods (NMDS, Kruskal, 1964, distance Bray-Curtis). The analysis was
222 carried out with metaMDS within R *vegan* (Oksanen et al., 2013), using a Wisconsin double
223 standardization and a maximum number of 100 runs to reach the best solution (two axis). To
224 visualize relationships between plant communities and environmental parameters, the resulting
225 NMDS biplot was interpreted using a post-hoc correlation with significant soil and environmental
226 parameters (function envfit).
227

3 Results

3.1 Patterned ground surface morphology and activity indicators.

The analyzed patterned ground features belonged to irregular reticulate fields. They showed almost bare centers and better vegetated margins (Table 2). In the barren parts of all the considered patterned ground features many plants were uprooted and small pebbles were heaved at the time of sampling.

In particular, on calcschist (CS site, Figure 2a), the patterned ground consisted of nonsorted circles of 0.8-2 m in diameter, with well vegetated rims surrounding bare central frost boils, which were slightly protruding from the surface. They were covered by a thin black cryptobiotic crust, often discontinued by tension cracks and fresh extrusions of fine soil materials caused by recent cryoturbation.

On serpentinite (SP site, Figure 2b), the patterned ground area consisted of large sorted stripes developed on a large gelifluction sheet, having a 1-2 m width and a few tens of metres of length. Sorted stripes and rock streams were associated with the gently sloping plateau (Table 1). The stony borders were made of blocks and cobbles (mostly between 7 and 30 cm), with many vertical or subvertical flagstones. They showed clear evidences of active movement, such as weak weathering rinds and few lichens located on random faces. The central area had a visible concentration of fine pebbles on the surface, and it was normally slightly protruding above the stony borders..

On metamorphic gabbros (GB site, Figure 2c), the almost flat surface was covered by a net of elongated sorted circles and polygons with a diameter between 1.2 and 3 m. The stony borders were slightly protruding above the low-lying central parts, and were made of large (10-30 cm) cobbles and flagstones and many verticalized slabs. The upper part of the largest stones was often covered by lichens, evidencing a weak activity of the borders associated with the development of dwarf shrub vegetation. Small pebbles were covering large proportions of the central surfaces.

252 On gneiss (GN site, Figure 2d), the patterned ground consisted in a net of sorted circles with a
253 diameter commonly between 1.2 and 2.5 m. The stony borders were 20-40 cm tall round ridges
254 raised above the central flat fine areas, and were made of subrounded, 5-20 cm pebbles and cobbles.
255 A surface redistribution of small pebbles into small circles was observed in the bare central parts of
256 many circles. A strong activity was verified by the absence of lichens on the stones of the borders.
257

258 *3.2 Soil morphology, mineralogy and texture.*

259 The studied soil profiles showed rather consistent morphological properties, such as horizonation,
260 active cryoturbation evidences and texture (Table 2, Table 3, Figure 3). Only minor mineralogical
261 variations were observed across the transects, with primary minerals dominating the clay fraction,
262 and a higher abundance of phyllosilicates, particularly serpentine, in the clay fraction than in the
263 coarse sand (Table 4). Pedogenic mica-vermiculite interlayered minerals were only detected in GN
264 samples.
265 The considered soils could be classified as Skeletic Eutric Regosols (Turbic), or Skeletic Eutric
266 Cambisol (Turbic) (GN site, according to IUSS Working Group, 2014), as A, AC, CA, C and C@
267 horizons were observed in all soils, only GN site had a morphological Bw. The WRB symbol @,
268 indicating cryoturbation, was used only for deep horizons showing a particularly strong platy
269 structure with vesicular pores and a very hard consistence, even if cryoturbation characterized most
270 horizons. In fact, active cryoturbation was manifested by irregular and broken horizon boundaries,
271 involutions and silt caps on the upper surfaces of stones (Bockheim and Tarnocai, 1998). C@
272 horizons were very similar to the overlying C, but had a harder consistence and a thicker platy
273 structure. Only the A horizons had a different structural aggregation, and were granular (in CS and
274 GB) or loose; these organo-mineral horizons were thickest close to the borders of the patterned
275 ground features.

As visible in Figure 3, a strong small-scale lateral variability characterized the selected patterned ground soils, with less developed horizons closer to the surface in the central parts and thicker A horizons close to the stony or vegetated rims.

In the surface layers, the texture was usually dominated by coarse sand in the outer portions of the features, with the smallest coarse sand contents in the central part, while silt showed the opposite trend (Table 2, Figure 4). Only CS samples had higher coarse sand and lower silt in the central part of the nonsorted circles than in the outer samples. Clay and fine sand did not change significantly across the features. A pronounced textural differentiation existed between surface A/AC/CA horizons and the underlying C and C@, but with different trends on the different parent materials. In SP and GB, the deep C and C@ horizons had a finer texture and a higher silt and clay content compared the surface ones (Table 3). In these soils, clay ranged from ca. 8-9% in surface layers to ca. 14-15% in deep C and C@. In GN, the finest texture was measured in the Bw, while silt and clay (not shown) were particularly low in the deep C@. In particular, in GN, clay content varied from 3.1% in the A, to 10.6% in the Bw, to 4.5% in the C and C@ horizons. Deep CS samples were characterized by a coarser texture, compared with the overlying horizons.

3.3 Soil chemical properties.

The chemical data of the main genetic horizons are shown in Table 3. Soil reaction was always acidic, also on base-rich parent materials. A very large small-scale variability of chemical properties was observed in the surface soil layers (Table 5): the TOC content was low in the central part of the patterns, and increased towards the rims, and this spatial pattern was reflected in most of the other chemical properties. In fact, pH values were the lowest and exchangeable bases were the highest in the most TOC-rich surface sectors. On SP, exchangeable Ni had the same trend as Ca and Mg. In CS nonsorted circles, Ni increased from south to north, in relation with a slightly higher serpentine content in the northern part. Nutrients generally followed the same trend as exchangeable bases and

TOC across the transects: in fact, the highest total N and available P were measured in the TOC-rich borders. Only in GN, available P had higher concentrations in the bare, TOC-poor central samples than in the rim ones. On gneiss, the overall P concentrations were however much higher than in the other sites.

As expected, the single chemical property characterizing all CS samples was a high exchangeable Ca (Figure 5a). In SP samples, a larger TOC accumulation was observed close to the stony borders than on the other parent materials. GB and SP samples had low Ca/Mg molar ratios (Figure 5b), while SP was characterized by high exchangeable Mg (not shown), a very high exchangeable Ni (5c) and less acidic soil reaction (Figure 5d). Very low Ni was measured in GB and GN sites. CS samples had intermediate levels of exchangeable Ni. Low TOC content, pH values and exchangeable bases (Table 5) were measured in GN. The C/N ratio, commonly used indicator of organic matter quality and decomposability, did not change significantly across the patterned ground transects nor across lithological variations of parent materials. Particuarly low values characterized GN samples, but were associated with N contents close to the analytical detection limit.

3.4 Vegetation and soil-vegetation relationships.

The vegetation in the sampling sites belonged to different phytosociological associations (Table 6). In particular, most plants growing on the nonsorted circles on CS were typical of humid soils with a long-lasting snow cover (*Salicetea herbaceae*). SP subplots were dominated by species normally associated to the *Thlaspietea rotundifolii* on basic scree soils, while GB and GN species were typical of different habitats (acidic scree, acidophilous grassland and humid soils with long-lasting snow cover). A slightly higher number of species sometimes characterized the better vegetated rims of the patterned ground features compared to the bare centres.

The cluster analysis (Figure 6a) was able to discriminate plant micro-communities developed on the different parent materials; the bare central areas were normally grouped with the associated well vegetated borders (with the exception of subplot GB-C, representing the centre of the sorted elongated circle on gabbros, associated with CS subplots). Inside the clusters, the rim vegetation was weakly separated from the central one in CS and GN sites. Also ordination methods (NMDS, Figure 6b) visually separated the plant micro-communities developed on the different parent materials, but did not separate the different sectors of the single patterned ground features.
The fitting of soil chemical variables on the NMDS biplot evidenced a significant correlation of plant community distribution with Ni, C/N ratio and a weakly significant one with Ca and P (Table 7), which were differential edaphic properties on the different substrata.

4 Discussions

4.1 Patterned ground, cryoturbation and short-range pedogenesis on different rock types

On the Alps, patterned ground environments are known to occur mostly in regions dominated by sedimentary rocks, where the regolith contains large quantities of fine materials, while it is only sporadic on crystalline rocks where blocks dominate the ground surface (Matsuoka et al., 1997). However, sedimentary rock outcrops are sporadic on the Western Alps, but patterned ground is commonly observed where the surface topography is sufficiently flat. Also in other mid-latitude mountain ranges, well developed patterned ground features are commonly observed on crystalline bedrocks (e.g. Munroe, 2007).
A strong, active cryoturbation characterizes the selected patterned ground areas, as demonstrated by many morphological indicators on the soil surface (absence or very few lichens on random faces of stones, uprooted plants, cracks in the cryptobiotic crust, extrusion of mud observed in spring in CS, GB and SP sites) and in the pedogenic horizons. Frost churning in the central part of the analyzed patterns was evidenced by convoluted horizon boundaries, while the thinner and less weathered

materials (corresponding to CA@ and C@ horizons) demonstrated upwelling from deeper depths caused by cryoturbation. Silt caps were observed in subsurface horizons in all soils, and were caused by either pervection (downward movement of silt particles through the profile associated with water movement during frost melting, Ugolini, 1986) or by the pressure created during the growth of ice lenses and/or the compression during the seasonal two-directional freezing of the active layer (Ugolini et al., 2006). The platy structural aggregation with abundant vesicular pores in subsurface horizons was likely caused by the growth of ice lenses during the two-directional autumn freezing, while needle ice formation and, possibly, a weak bioturbation were associated with the fine granular or loose aggregation of surface layers (Ping et al., 2008). The large diameter of many stones in the borders and the almost complete absence of lichens on them showed that cryoturbation is deep and presently active, and probably associated with permafrost (Goldthwait 1976) in agreement with the temperature and site indicators shown in section 2.1.

Few active cryoturbated soils have been observed in mid-latitude mountain areas, also above permafrost, likely because of a deep (1-8 m) active layer and a reduced water content (Bockheim and Munroe, 2014). In the considered soils, however, water availability should not limit an abundant ice lens formation during autumn freeze-back and cryoturbation (see section 2.1).

One effect of cryoturbation was the pronounced textural differentiation between horizons and across the transects of the patterns. In fact, the bare central parts were strongly enriched in silt (up to more than 20% of variation from the rims) and impoverished in coarse sand. These data were similar to the silt plus clay trend observed in some sorted circles developed in other mid-latitude mountain ranges (Rocky Mountains, Harris, 1990), in arctic tundra (Kling ,1996) or in cold desert soils (Ugolini et al., 2006). A strong vertical sorting of particle sizes was also detected, with dense C and C@ horizons particularly rich in silt and poor in coarse sand, as a result of either pervection or cryo-ejection of the coarse fraction towards the surface (Ugolini et al., 2006) caused by cryoturbation. Pervection is facilitated during frost melt, which causes a disruption of structural aggregates in surface layers and permits an easy translocation of silt particles at depth with melt and rainwater.

376 The opposite lateral and depth trends of silt and coarse sand were measured in the CS nonsorted
377 circles. This might be related to a different weathering regime characterizing carbonate-rich
378 materials, as the carbonate cements readily dissolve in the surface layers under the acidifying
379 conditions characterizing these humid high alpine environments and because they are not strong
380 enough to resist the physical stress imposed by cryoturbation and frost churning. In fact the first
381 visible effect of parent material is the presence or absence of stony borders: on easily physically
382 weatherable calcschist, nonsorted circles and frost boils (and earth hummocks at lower altitude)
383 dominate flat surfaces, while sorted circles or stripes are developed on more resistant lithotypes.
384 Cryoturbation also influences the lateral distribution of most chemical properties, which derives
385 directly from the soil movements associated with freeze-thaw cycles (which is related with soil
386 circulation, cryogenic mass exchange, plant uprooting and vegetation cover disruption), but also
387 it is indirectly related with the presence of weakly weathered and highly weatherable C horizon-
388 like materials close to the soil surface in the central parts. As a result, topsoil TOC content was
389 much higher near the rims than in the central parts, thanks to the higher plant cover, the weaker
390 cryoturbation normally characterizing the stone-rich rims of sorted patterned ground and the
391 vegetated borders of nonsorted features, and thanks to the outward movement of fine surface
392 particles observed in the centre of patterned ground features (e.g. Matsuoka et al., 2003). This
393 trends correspond to increasingly better developed A horizons towards the rims. Correlated with
394 the higher TOC content and the higher surface stability (which favored leaching) characterizing
395 the rims, pH values decreased of more than one point from the disturbed, cryoturbated centers to
396 the rims (Table 4). Conversely, exchangeable bases and nutrients (N and P) decreased from the
397 rims to the centers, because of the higher CEC, biocycling and bioaccumulation in TOC-rich
398 sectors. These results confirm the importance of bioaccumulation on cold tundra soils, as already
399 noticed in the Arctic (Michaelson et al., 2008). P concentration had the opposite trend along the
400 GN transect, with highest contents measured in the bare and TOC-poor central subsamples. In
401 GN samples, overall P contents were higher than in the others, thanks to the high total P included

in sialic gneisses and granites (Porder and Ramachandran, 2013). Both trends have been already observed in arctic patterned ground soils, but this difference was not explained by primary P content in the parent materials (e.g., Broll et al., 1999; Walker et al., 2004 found higher available P in the TOC-rich border, while Jonasson and Sköld, 1983, found the opposite trend). From our results it seems likely that P biocycling and bioaccumulation in TOC-rich horizons is important on P-poor substrates, while early weathering of P-bearing primary minerals is important in P availability on P-rich substrates in these cold soils.

Cryptobiotic crusts are known to be rich in N-fixing cyanobacteria, and are important N sources in otherwise nutrient-poor polar deserts (e.g., Dickson 2000), but in the observed patterned ground N was not higher in crusted CS than in the other, non-crusted sites. Moreover, the high C/N ratio (ca. 19) in the crust evidences that N is not accumulated in this surface soil layer. P bioaccumulation, however, was evident in the cryptobiotic crust, as often observed in frost boils (Michaelson et al., 2012).

Despite this wide small-scale spatial variability in chemical properties primarily caused by cryoturbation, which likely have strong impacts on small-scale soil ecology, the differences caused by the different parent materials were overwhelming, as shown by the significant differences in exchangeable bases, heavy metals and available P between the considered patterned ground soils.

In particular, GN samples had the highest available P and the lowest exchangeable bases, CS had high exchangeable Ca and Ca/Mg molar ratios, SP had high exchangeable Ni and pH values, SP and GB had low Ca/Mg molar ratios. A low Ca/Mg ratio normally characterizes serpentine soils, and is one of the factors normally creating stress for non-adapted plant species (Brooks, 1987). In the considered soils, this parameter changed only slightly both between the different substrates and along the transects, uncorrelated to TOC despite the frequent selective bioaccumulation of Ca in Mg-rich soils (e.g., D'Amico and Previtali 2012). The high exchangeable Ni content in SP was likely contributing to the low decomposition rate of organic matter, evidenced by the

428 exceptional TOC accumulation on the stony rims, already detected in the area and not correlated
429 with a particularly high vegetation cover, comparable to that of the GN site and much lower than
430 in CS. In the same alpine ophiolitic outcrop, labile forms of heavy metals were significantly
431 correlated with stress indicators for microbial communities (D'Amico, 2009).
432 In general, pedogenesis in these soils is dominated by a differential organic matter accumulation
433 in relation with the scant plant cover distribution and by acidification: while high-latitude
434 habitats are characterized by dry climates, and carbonates and soluble salts accumulate in the
435 surface and subsurface soil horizons (e.g., Ugolini et al., 2006; Walker et al., 2004), in alpine
436 areas the abundant precipitation increases leaching, and soils are quickly acidified also on
437 carbonate-rich or basic/ultrabasic parent materials. Low pH values were observed also in the
438 central, bare sectors of the patterned ground features, even if the mineralogy was dominated by
439 primary unweathered minerals.
440

441 *4.2 Vegetation and short range soil-vegetation relationships*

442 A common characteristic of the plant communities in the observed patterned ground areas was
443 the stress caused by late summer freezing, which caused a widespread uprooting of the plants
444 growing in the central parts of the patterns, without strong distinction between crusted sites (CS
445 site) and non-crusted ones (differently from what reported for arctic desert patterned ground by
446 e.g. Anderson and Bliss, 1998). As usual, plant cover was higher near the rims of sorted and
447 nonsorted features, thanks to the higher stability of these portions (verified on the field, as plants
448 were not uprooted in the rim micro-habitat). The barren aspect of high altitude alpine
449 environments is indeed caused by soil instability, which is strongly associated with climate
450 severity, as it normally happens in cold polar desert habitats, even if the latter is characterized by
451 much colder air temperatures, particularly during winter months. In high altitude, mid-latitude
452 mountain ranges, the climatic harshness is probably associated with a high number of diurnal

freeze-thaw cycles and needle ice formation during snow-free periods, which impose a stress on plant roots, together with excessive drainage (Bliss, 1956).

Despite a similar general appearance of the selected patterned ground areas, each site was colonized by different plant communities, with only few species in common and without a significant differentiation between the central part and the rims on each substrate, as already detected in similar habitats on the Alps (Gerdol and Smiraglia, 1990; Béguin et al., 2006). Differently from the similar vegetation observed on active patterned ground on the Alps, in subarctic and arctic tundra sites the barren patterns centers were covered by scattered basophilous, stress-tolerant herbs, while the more stable and acidified rims were colonized by dwarf acidophilous heath species, less tolerant to cryogenic soil disturbances. (e.g., Jonasson and Sköld, 1983; Jonasson, 1986; Anderson and Bliss,1998; Cannone et al., 2004).

A reason possibly explaining the lack of vegetation differentiation between rims and centers in active patterned ground in high altitude, mid-latitude mountain ranges could be the high substrate specificity of alpine plant communities (e.g., D'Amico and Previtali, 2012). The strong association of different species associations with specific chemical properties overran the stability and edaphic gradients observed within the single patterned ground features. In a more generalized work concerning edaphic influences on vegetation (D'Amico and Previtali, 2012), the plant communities growing on active patterned ground (close to CS, SP and GB sites) were grouped with substrate-specific high altitude communities, which appeared well correlated with chemical properties characteristic of each substrate lithology. Cryoturbation was not an important factor in alpine vegetation differentiation.

While CS site had a rather hygrophilous vegetation, likely thanks to the humidity characterizing this soil with a rather fine granulometry, the plant communities on the other sites were associated with specific, substrate-inherited chemical properties (Table 7, Fig. 5, Fig. 6). High exchangeable Ni was significantly correlated with the serpentine community, as already observed in alpine ophiolitic soils, and SP vegetation, in fact, included one Ni-hyperaccumulator (*Thlaspi*

rotundifolium subsp. *corymbosum*) and one serpentine endemic (*Carex fimbriata*), which are normally well correlated with high exchangeable Ni on alpine serpentine soils (D'Amico and Previtali, 2012; D'Amico et al., 2014). High exchangeable Mg and a low Ca/Mg molar ratio, normally characteristic of serpentine soils and important causes of stress for non-adapted plant species (Brooks, 1987), were not correlated with plant communities in the study sites.

Total vegetation cover was not related to soil nutrients or, apparently, to other chemical parameters, but to low temperatures, as demonstrated by the lowest cover value in the site (GN) located at the highest elevation, even if it was particularly rich in available P. In less climate-limited ecosystems at the subalpine phytoclimatic belt, available P was the single chemical element involved in differentiating barren surfaces from well vegetated ones, in nearby ophiolitic areas (D'Amico et al., 2014). Similarly, average temperature is an important driver in ecosystem productivity and in the patterned ground habitat functioning also in Arctic frost boil environments, where it influences the mutual relationships between frost heave, vegetation colonization and soil properties (Walker et al., 2004).

5 Conclusions: mid-latitude alpine patterned ground ecological functioning

The climate conditions characterizing high alpine, mid latitude mountain areas, with short growing seasons, the climate factor (with frequent daily freeze-thaw cycles during snow-free periods, long winters with strong winds locally removing the thick snow cover thus reducing its protective effect on vegetation and soil) is a strong constraint against plant colonization (Figure 7). In these areas, where plant cover is scarce and winds remove snow during winter, deep seasonal freezing and permafrost conditions are able to create a strong soil cryoturbation, leading to the formation of well developed patterned ground features, on limited flat or gently sloping surfaces. Patterned ground features can be sorted or nonsorted, based on the parent material liability to physical frost shattering and chemical weathering. Both sorted or nonsorted features

504 are characterized by widely variable edaphic conditions, related with small-scale vegetation
505 cover differences associated with different levels of cryogenic surface disturbances. In particular,
506 low TOC, exchangeable bases and nutrients, and potentially toxic heavy metals are measured in
507 the bare central sections, and higher concentration of the same substances are found on the more
508 stable, better vegetated rims. Plant-available phosphorus is concentrated in TOC-rich horizons
509 near the rims, thanks to biocycling and increased Cation Exchange Capacity (normally correlated
510 with the organic matter), except on particularly P-rich substrates (i.e., gneiss), where it is mostly
511 associated with the early weathering of fresh, P-rich minerals; on P-rich materials, the highest
512 available P levels are measured in the bare central parts. Edaphic properties inherited from the
513 parent rocks, including heavy metals, exchangeable Ca and Ca/Mg molar ratio are the factors
514 which differ most between soils formed on different parent rocks, with differences far
515 outweighing the intra-pattern variability. These chemical factors are also associated with the
516 different plant species colonizing patterned ground habitats developed over different parent
517 rocks. In particular, high exchangeable Ni characterizes serpentine soils, and it is strongly
518 associated with a specific vegetation which includes endemic and Ni-hyperaccumulating species.
519 High precipitation rates (>1200 mm/y) increase leaching of carbonates, so that most of the plant
520 species growing on these cryoturbated soils are typical of acidic substrates, also on carbonate-
521 rich materials such as calcschists.
522
523 **Acknowledgments**
524 This research was supported by the Italian MIUR Project (PRIN 2010-11; grant number
525 2010AYKTAB_006): “Response of morphoclimatic system dynamics to global changes and
526 related geomorphological hazards” (national coordinator C. Baroni).

527 **Literature**

528 Anderson, D.G., Bliss, L.C., 1998. Association of plant distribution patterns and
529 microenvironments on patterned ground in a polar desert. Arct. Alp. Res. 30, 97–107.
530 Ballantyne, C.K., 1996. Formation of Miniature Sorted Patterns by Shallow Ground Freezing: a
531 Field Experiment. Permafr. Perigl. Proc. 7, 409-424.
532 Ballantyne, C.K., 2013. Patterned ground. In: The Encyclopaedia of Quaternary Science. Second
533 Ed. Elsevier: Amsterdam, pp. 452-463.
534 Beguin, C., Progin Soney, M., Vonlanthen, M., 2006. La Végétation des sols polygonaux aux
535 étages alpine supérieur et subnival en Valais (Alpes centro-occidentales, Suisse). Bot. Helv. 116,
536 41-54.
537 Bliss, L.C., 1956. A comparison of plant development in microenvironments of arctic and alpine
538 tundras. Ecol. Monogr. 26, 303-337.
539 Bockheim, J.G., Tarnocai, C., 1998. Recognition of cryoturbation for classifying permafrost-
540 affected soils. Geoderma 81(3-4), 281-293.
541 Bockheim, J.G., Munroe, J.S., 2014. Organic carbon pools and genesis of alpine soils with
542 permafrost: a review. Arct. Antarct. Alp Res. 46(4), 987-1006.
543 Boeckli, L., Brenning, A., Gruber, S. Noetzli, J., 2012. Permafrost distribution in the European
544 Alps: calculation and evaluation of an index map and summary statistics, The Cryosphere 6, 807–
545 820.
546 Broll, D., Tarnocai, C., Mueller, D., 1999. Interactions between vegetation, nutrients and moisture
547 in soils in the Pangnirtung Pass Area, Baffin Island, Canada. Permafr. Periglac. Proc. 10, 265-277.
548 Brooks, R.R., 1987. Serpentine and its vegetation: a multidisciplinary approach. Dioscorides,
549 Oregon.
550 Cannone, N., Guglielmin, M., Gerdol, R., 2004. Relationships between vegetation patterns and
551 periglacial landforms in Northwestern Svalbard. Polar Biol. 27, 562-571.

552 D'Amico, M.E., 2009. Soil ecology and pedogenesis on ophiolitic materials in the western Alps
553 (Mont Avic Natural Park, North-western Italy): soil properties and their relationships with substrate,
554 vegetation and biological activity. PhD thesis, Università degli Studi di Milano Bicocca.
555 D'Amico, M.E., Previtali, F., 2012. Edaphic influences of ophiolitic substrates on vegetation in the
556 Western Italian Alps. Plant Soil 351, 73-95.
557 D'Amico, M.E., Freppaz, M., Leonelli, G., Bonifacio, E., Zanini, E., 2014. Early stages of soil
558 development on serpentinite: the proglacial area of the Verra Grande Glacier, Western Italian Alps.
559 J. Soils Sedim. DOI: 10.1007/s11368-014-0893-5.
560 Dickson, L.G., 2000. Constraints to nitrogen fixation by cryptogamic crusts in a polar desert
561 ecosystem, Devon Island, NWT, Canada. Arct. Antarct. Alp. Res. 32, 40-45.
562 Etzelmüller, B., Sollid, J.L., 1991. The role of weathering and pedological processes for
563 development of sorted circles on Kvadehuksletta, Svalbard - a short report. Polar Res. 9(2) (1991),
564 181-191
565 FAO, 2006. Guidelines for Soil Description, 4th ed. FAO, Rome.
566 Feuillet, T., 2011. Statistical Analyses of Active Patterned Ground Occurrence in the Taillon Massif
567 (Pyrénées, France/Spain). Permafr. Periglac. Proc. 22, 228-238.
568 Gerdol, R., Smiraglia, C., 1990. Correlation between vegetation pattern and micromorphology in
569 periglacial areas in the Central Alps. Pirineos 135, 13-28.
570 Goldthwait, RP., 1976. Frost sorted patterned ground: a review. Quat. Res. 6, 27-35.
571 Harris, C., 1990. Micromorphology and microfabrics of sorted circles, Front Range, Colorado,
572 U.S.A. Nordicana 54, 89-94.
573 Harris, C., Arenson, L.U., Christiansen, H.H., Etzelmüller, B., Frauenfelder, R., Gruber, S.,
574 Haeberli, W., Hauck, C., Hölzle, M., Humlum, O., Isaksen, K., Kääb, A., Kern-Lütschg, M.A.,
575 Lehning, M., Matsuoka, N., Murton, J.B., Nötzli, J., Phillips, M., Ross, N., Seppälä, M., Springman,
576 S.M., Vonder Mühll, D., 2009. Permafrost and climate in Europe: monitoring and modeling
577 thermal, geomorphological and geotechnical responses. Earth-Sci. Rev. 92, 117-171.

578 Haugland, J.E., 2004. Formation of patterned ground and fine-scale soil development within two
579 late Holocene glacial chronosequences: Jotunheimen, Norway. Geomorphology 61, 287-301.
580 Haugland, J.E., Owen, B.S., 2005. Temporal and spatial variability of soil pH in patterned ground
581 chronosequences: Jotunheimen, Norway. Phys. Geogr. 26 (4), 299-312
582 Hothorn, T., Bretz, F., Westfall, P., 2008. Simultaneous Inference in General Parametric Models.
583 Biometrics J. 50 (3), 346–363
584 Imhof, M., Pierrehumbert, G., Haeberli, W., Kienholz, H., 2000. Permafrost investigations in the
585 Schilthorn Massif, Bernese Alps, Switzerland. Permafr. Perigl. Proc. 11, 189-206.
586 Johnson, P.L., Billings, W.D., 1962. The alpine vegetation of Beartooth Plateau in relation to
587 cryopedogenic processes and patterns. Ecol. Monogr. 32 (2), 105-135.
588 Jonasson, S., Sköld, S.E., 1983. Influences of frost-heaving on vegetation and nutrient regime of
589 polygon-patterned ground. Vegetatio 53 (2), 97-112
590 Jonasson, D., 1986. Influence of frost heaving on soil chemistry and on the distribution of plant
591 growth forms. Geografiska Annaler. Series A, Phys. Geogr. 68(3), 185-195.
592 Kling, J., 1996. Relict sorted patterned ground in Rostu, Northernmost Sweden. Geografiska
593 Annaler. Series A, Phys. Geogr. 78 (1): 61-72.
594 Körner, C., 2003. Alpine Plant Life. Springer-Verlag, Heidelberg and New York, 338 pp.
595 Kruskal, J.B., 1964. Nonmetric multidimensional scaling: a numerical method. Psychometrika 29,
596 115-29.
597 Matsuoka, N., Hirakawa, K., Watanabe, T., Moriwaki, K., 1997. Monitoring of periglacial slope
598 processes in the Swiss Alps: the first two years of frost shattering, heave and creep. Permafr.
599 Periglac. Proc. 8, 155-177.
600 Matsuoka, N., Abe, M., Ijiri, M., 2003. Differential frost heave and sorted patterned ground: field
601 measurements and a laboratory experiment. Geomorphology 52, 73–85,
602 Mercalli, L., 2003. Atlante climatico della Valle d'Aosta. Società Meteorologica Italiana, Torino.

603 Mercalli, L., Cat Berro, D., 2005. Climi, acque e ghiacciai tra Gran Paradiso e Canavese. Ed.
604 Società Meteorologica Subalpina, Bussoleno (To, Italy).
605 Michaelson, J.G., Ping, C.L., Epstein, H., Kimble, J.M., Walker, D.A., 2008. Soils and frost boil
606 ecosystems across the North American Arctic Transect. J. Geophys. Res. 133, G03S11.
607 Michaelson, J.G., Ping, C.L., Walker, D.A., 2012. Soils Associated with Biotic Activity on Frost
608 Boils in Arctic Alaska. Soil Sci. Soc. Am. J. 76 (6), 2265-2277.
609 Munroe, J.S., 2007. Properties of Alpine Soils Associated with Well-Developed Sorted Polygons in
610 the Uinta Mountains, Utah, U.S.A. Arct. Antarct. Alp. Res. 39 (4), 578–591.
611 Oksanen, J., Guillaume Blanchet, F., Kindt, R., Legendre, P., Minchin, P.R., O'Hara, R.B.,
612 Simpson, G.K., Solymos, M.P., Stevens, H.H., Wagner, H., 2013. vegan: Community Ecology
613 Package. R package version 2.0-8. http://CRAN.R-project.org/package=vegan.
614 Pignatti, S., 1992. Flora d'Italia, vol 1–3. Edagricole, Bologna
615 Ping, C.L., Michaelson, G.J., Kimble, J.M., Romanovsky, V.E., Shur, Y.L., Swanson, D.K.,
616 Walker, D.A., 2008. Cryogenesis and soil formation along a bioclimate gradient in Arctic North
617 America. J. Geophys. Res. 113, G03S12
618 Porder, S., Ramachandran, S.. 2013. The phosphorus concentration of common rocks - a potential
619 driver of ecosystem P status. Plant Soil 367, 41-55.
620 Ugolini, F.C., 1966. Soils of the Mesters Vig District, northeast Greenland: I. The Arctic Brown
621 and related soils. Meddelelser om Grønland 176, 1–22.
622 Ugolini, F.C., 1986. Pedogenic zonation in well-drained soils ot the Arctic regions. Quat. Res. 26,
623 100-120.
624 Ugolini, F.C., Corti, G., Certini, G., 2006. Pedogenesis in the sorted patterned ground of Devon
625 Plateu, Devon Island, Nunavut, Canada. Geoderma 136, 87-106.
626 Van Reeuwijk, L.P., 2002. Procedures for Soil Analysis. Technical Paper n. 9. International Soil
627 Reference and Information Centre. Wageningen, Netherlands.

628 Walker, D.A., Epstein, H.E., Gould, W.A., Kelley, A.M., Kade, A.N., Knudson, J.A., Krantz, W.B.,
629 Michaelson, G., Peterson, R.A., Ping, C.L., Raynolds, M.K.. Romanovsky, V.E., Shur, Y., 2004.
630 Frost-Boil Ecosystems: Complex Interactions between Landforms, Soils, Vegetation and Climate.
631 Permafr. Periglac. Process. 15, 171–188.
632 Washburn, A.L., 1980. Permafrost features as evidence of climatic change. Earth Sci. Rev. 15, 327-
633 402.
634

Figure 1: The location in the North-western Italian Alps and extracts from the Alpine Permafrost Index Data (Boeckli et al., 2012) showing the high probability of permafrost in the elected sites.

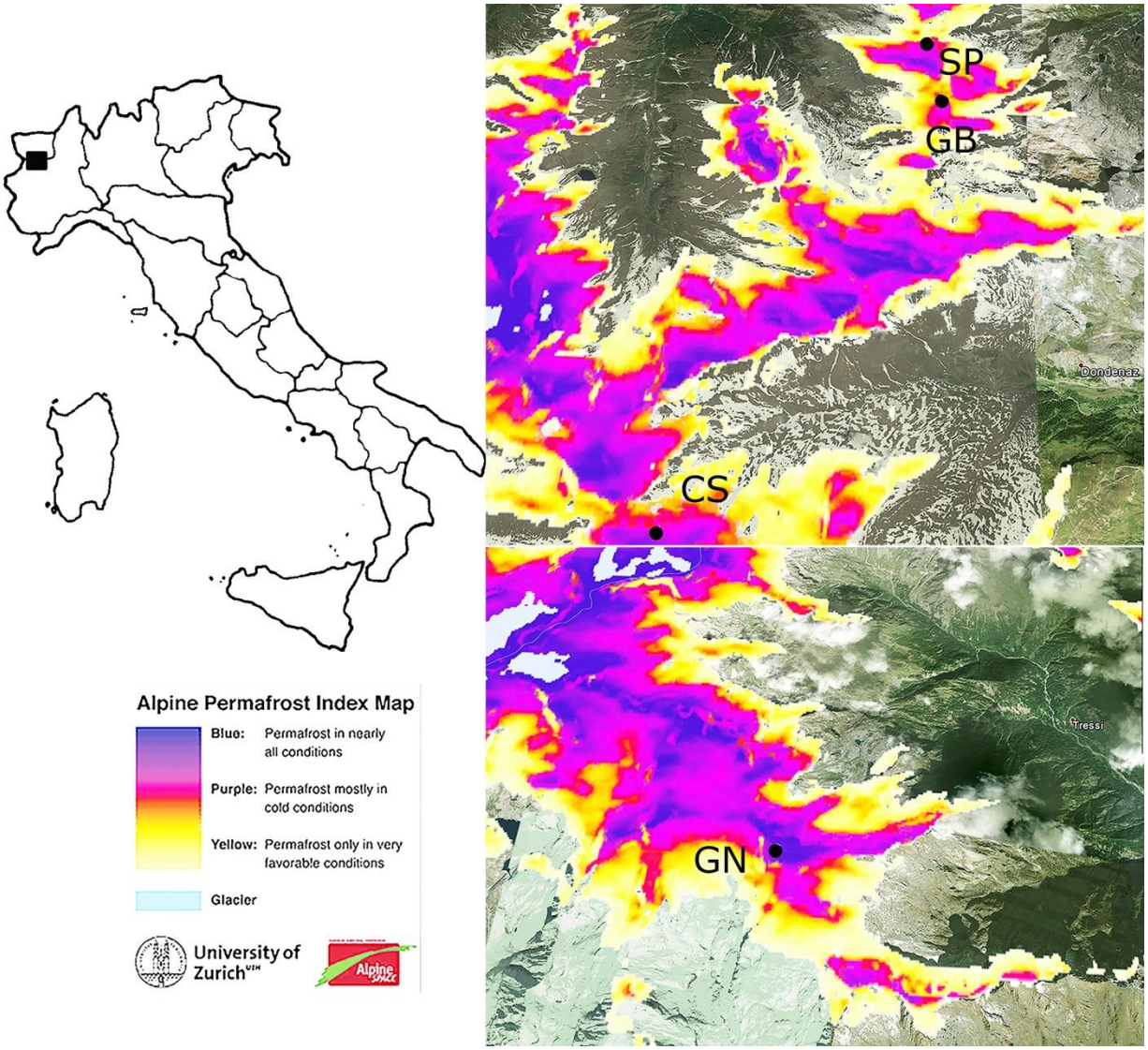

639 Figure 2: Views of the selected alpine patterned ground habitats.

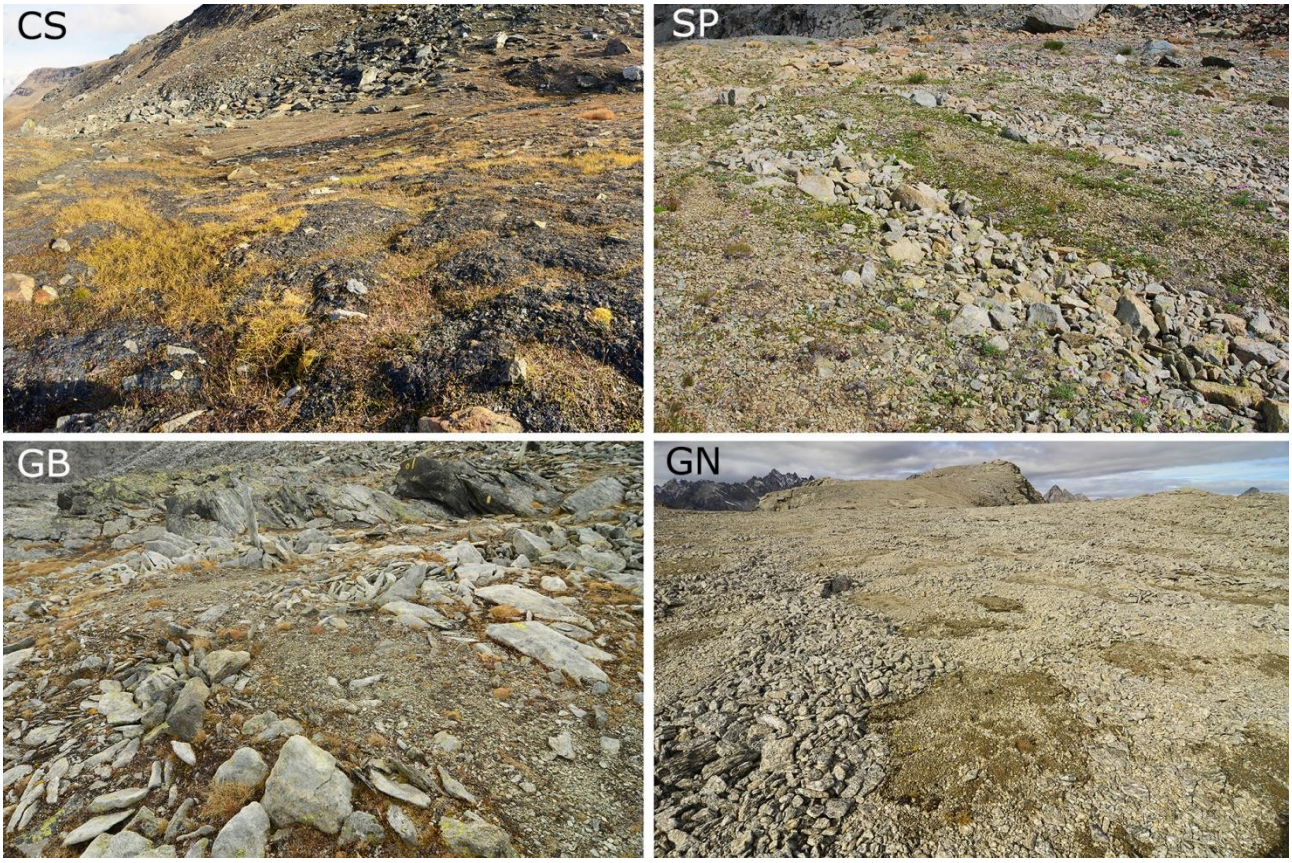

640

641

Figure 3: horizon limits and distribution across the selected active patterned ground features. From top to bottom, sections across the nonsorted circle on calcschists (CS site), and across the sorted stripes on serpentinite (SP site), the sorted elongated circles on gabbros (GB site) and the sorted circles on gneiss (GN site).

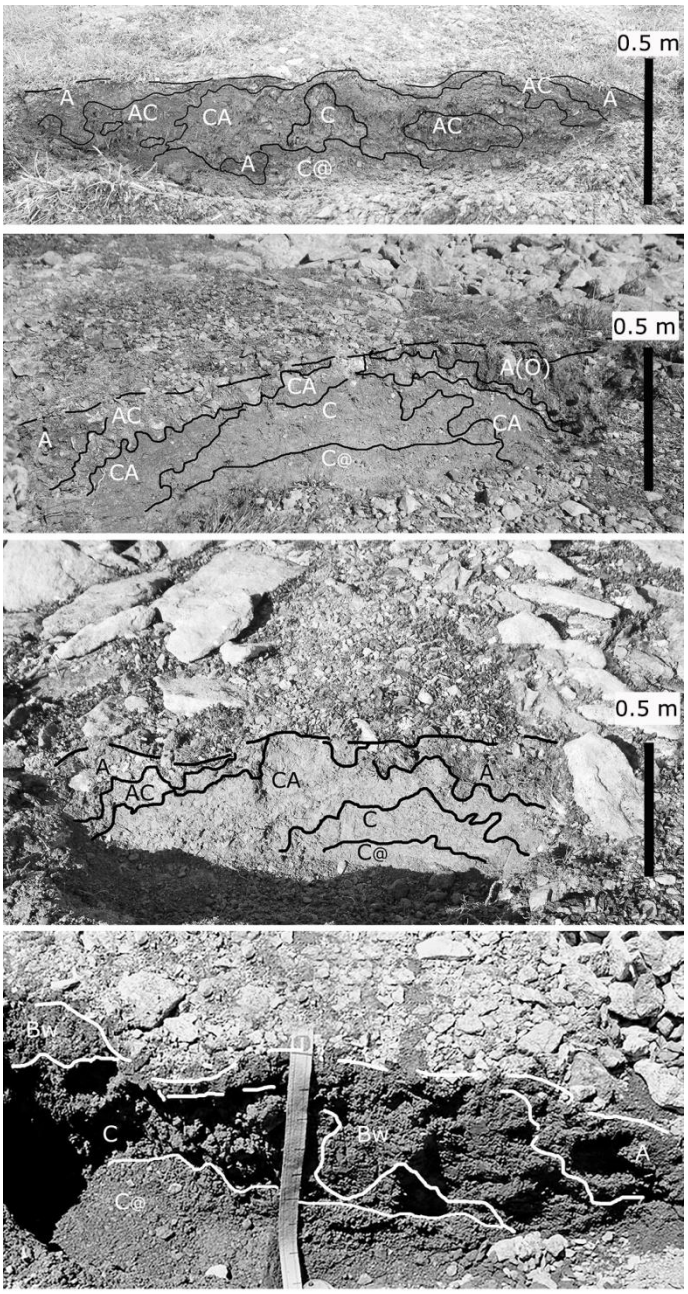

Figure 4: coarse sand (a) and silt (b) contents in the fine earth of surface layers across the studied patterned ground transects.

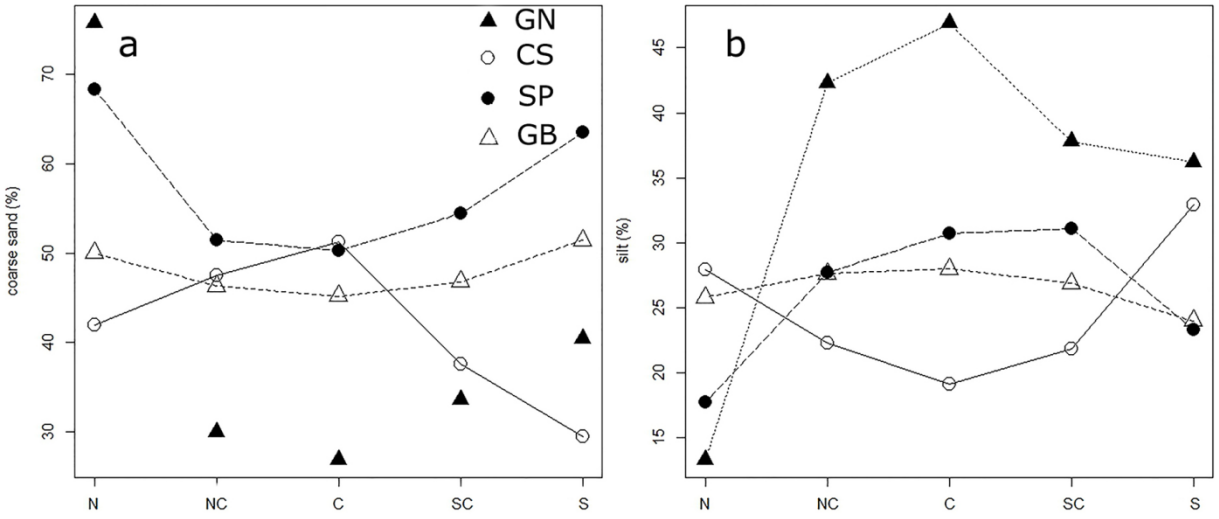

Figure 5: Some significantly different chemical properties associated with specific parent materials: Ca (a), Ca/Mg molar ratio (b), Ni (c) and pH values (d).

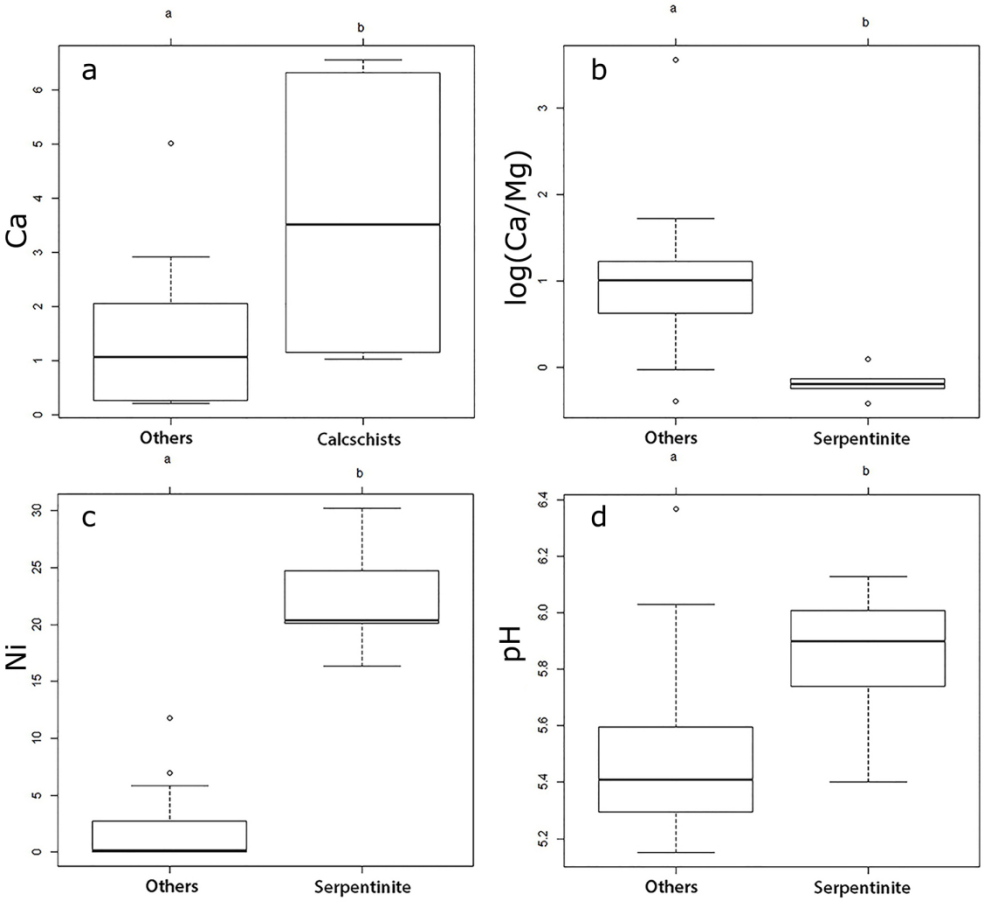

Figure 6: Cluster dendrogram (a) and NMDS ordination biplot, with fitted pedo-environmental variables (b), of the vegetation growing along the transects of the selected patterned ground features. The numbers 1, 2, 3, 4 before the position identification code represent, respectively, the CS, SP, GB and GN sites.

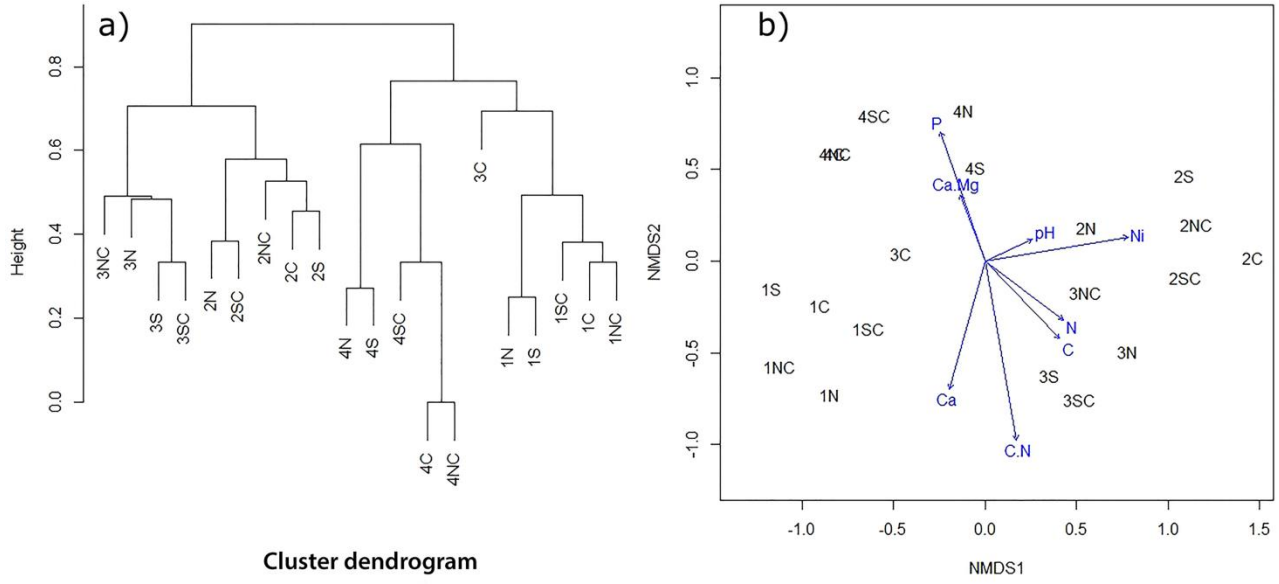

661 Figure 7: Conceptual diagram of patterned ground functioning in the Italian Western Alps; full
662 lines indicate strong relationships directly derived from the results of study, dotted lines indicate
663 known relationships whose effects cannot be directly evidenced.

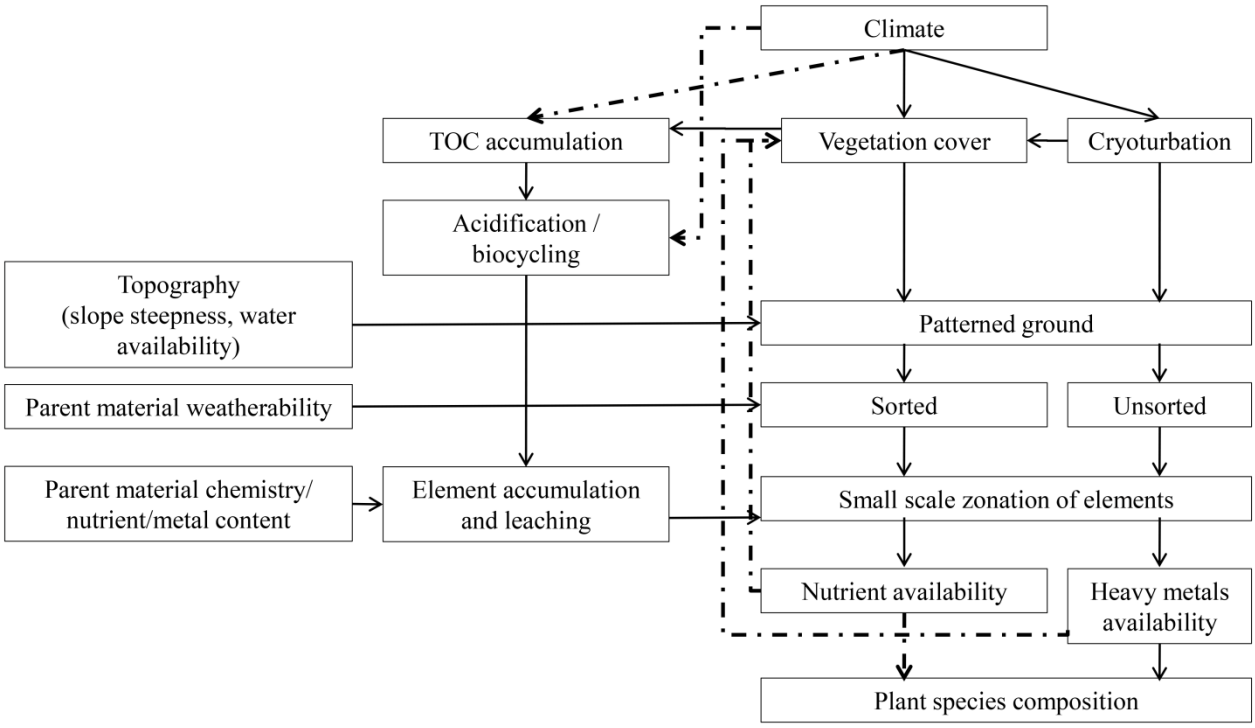

664

665

666

667 Table 1: localization and environmental properties of the study sites

	Coordinates	**Parent material**	**Elevation (m a.s.l.)**	**Slope angle**	**Patterned ground type**	**Dimensions (m)**	**Aspect**	**WRB (FAo-ISRIC, 2014)**
CS - Fenetre de Champorcher (Champorcher, AO)	45°35'57.41", 07°30'18.90"	Calcschists (serpentinite in traces)	2705	1°	Nonsorted circles, hummocks	0.8/1.5	45°	Skeletic Eutric Regosols (Turbic)
SP - Colle di Raye Chevrere (Champdepraz, AO)	45°40'04.70" 07°32'31.32"	Serpentinite	2710	4°	Sorted stripes	0.8/1.5-3/8	45°	Orthoskeletic Eutric Regosols (Turbic)
GB - Lac des Heures (Champdepraz, AO)	45°29'36.14" 07°32'53.77"	Gabbro	2780	2°	Sorted elongated circles	1.2/2-2-2.5	90°	Orthoskeletic Eutric Regosols (Turbic)
GN - Piata Lazin (Ronco Canavese, TO)	45°29'21.74" 7°26'21.30"	Gneiss	3054	0°	Sorted circles	0.8/2	n.d.	Orthoskeletic Eutric Cambisol (Turbic)

668

669 Table 2: parameters of the surface samples along transects through the selected patterned ground
670 features.

Site	Lithology	Position along the transects / sample code	Vascular plant cover (%)	Bare soil cover (including cryptobiotic crust) (%)	Surface stoniness (%)	Cryptobiotic crust cover (%)	Coarse Sand (%)	Silt (%)	Clay (%)
CS	Calcschists (serpentinite in traces)	CS - S	100	0	10	0	42.0	27.9	10.1
		CS - SC	20	75	5	70	47.5	22.3	10.1
		CS - C	5	90	3	95	51.2	19.1	8.3
		CS - NC	30	65	5	60	37.6	21.8	8.9
		CS - N	98	0	5	0	29.5	32.9	9.3
SP	Serpentinite	SP - S	50	0	80	0	68.3	17.7	9.4
		SP - SC	20	40	50	0	51.4	27.7	8.3
		SP - C	5	50	40	0	50.3	30.7	8.6
		SP - NC	10	40	50	0	54.4	31.1	8.8
		SP - N	50	0	70	0	63.5	23.3	8.4
GB	Metamorphic gabbros	GB - S	30	5	80	0	50.0	25.8	10.0
		GB - SC	10	50	40	0	46.3	27.6	9.4
		GB - C	1	60	40	0	45.2	28.0	9.3
		GB - NC	5	50	45	0	46.8	26.9	9.4
		GB - N	40	0	80	0	51.4	24.0	9.3
GN	Gneiss	GN - S	5	0	100	0	75.7	13.3	7.0
		GN - SC	1	60	40	0	30.0	42.3	11.0
		GN - C	0	80	20	0	26.9	46.9	12.0
		GN - NC	1	60	40	0	33.6	37.8	8.0
		GN - N	5	0	100	0	40.4	36.2	8.9

671

672

673 Table 3: morphology and main chemical properties of the soil horizons observed in the patterned
674 ground soils, as shown in Figure 3.

Site	Horizon	Colour (mottles, colour and %)	Structure	Consistence	Silt caps[1]	Roots[2]	pH	TOC %	Exchangeable Ca cmol/kg	Exchangeable Ca/Mg molar ratio	Silt (%)	Coarse sand (%)
CS	O*	2.5Y 2/1			-	+++	5.3	8.73	6.42	3.23		
	A	2.5Y 2/1	Gr 1	Soft	-	++	5.5	3.08	9.11	5.9	31.1	35.6
	AC@	5Y 4/2 (2.5Y 2/1, 30%)	Pl 2	Slightly hard	-	+	5.7	0.81	8.08	6.6	22.1	42.2
	CA@			Slightly hard	-	-	5.9	0.78	6.89	7.2	25.6	33.9
	C@1	5Y 4/2	Pl 3	Slightly hard	++	-	6.4	0.72	4.21	7.8	18.3	52.1
	C@2	5Y 4/2	Pl-vs 3	Hard	++	-	6.5	0.68	3.91	6.7	17.9	53.2
SP	A(O)	2.5Y 3/2	SG	Loose	-	++++	5.4	11.81	5.02	1.1	17.7	68.3
	A	2.5Y 3/2	SG	Loose	-	++	6.0	3.11	1.31	0.9	23.3	63.5
	AC@	2.5Y 4/2	Pl-vs 3	Slightly hard	-	+	6.1	1.81	0.61	0.8	31.1	54.4
	CA@	5Y 4/2	Pl-vs 3	Hard	++	+	6.1	0.48	0.97	0.8	27.7	51.4
	C@1	5Y 5/2	Pl-vs 3	Hard	+++	-	6.6	0.13	0.33	0.5	33.0	46.6
	C@2	5Y 5/2	Pl-vs 4	Very hard	+++	-	6.6	0.12	0.29	0.4	29.1	41.2
GB	A	2.5Y 3/2	Gr 1	Soft	-	+++	5.2	6.18	2.58	1.3	24.7	50.7
	AC@	5Y 4/2	Pl vs 3	Slightly hard	-	+	5.3	2.43	1.15	2.1	27.3	46.5
	CA@	5Y 5/2	Pl vs 3	Hard	++	+	6.2	0.84	0.95	0.9	28.0	45.2
	C@1	5Y 5/2	Pl-vs 4	Hard	+++		6.4	0.42	1.39	0.8	34.1	39.6
	C@2	5Y 5/2	Pl-vs 4	Very hard	+++		6.5	0.39	1.45	0.8	35.6	42.3
GN	A	2.5Y 3/2	SG	Loose	-	+	5.3	0.62	0.24	3.2	13.3	75.7
	Bw@	10YR 4/3	Pl-vs 2	Soft	+	-	5.4	0.41	0.21	2.8	43.6	31.5
	C@1	2.5Y 4/3	Pl-vs 3	Hard	+++	-	5.7	0.31	0.19	2.0	35.5	29.1
	C@2	2.5Y 4/3	Pl-vs 4	Hard	+++	-	5.8	0.25	0.18	2.2	28.1	51.1

675 *: O horizon in CS soil is a cryptobiotic crust. Structure codes: Gr, granular; SG, single grain; Pl,
676 platy; vs, visible vesicular porosity; 1, weak; 2, moderate; 3, strong; 4, very strong aggregates. [1]:
677 quantity and thickness of silt caps on stone fragments: +++: observed on most stones, with

678 thickness > 1mm; ++: visible on most coarse clasts, but thinner; +: observed on some stones. [2]:

679 abundance of roots: ++++: abundant; +++: common; ++ scarce; +: very few.

680

Table 4: semiquantitative mineralogical composition, from XRD analysis of coarse sand and clay particles in surface S, C and N samples. ++++ correspondes to quantities higher than 66%, +++ corresponds to quantities between 33 and 66%, ++ corresponds to quantities between 5 and 33%, and + corresponds to trace amounts of minerals. - corresponds to undetected minerals.

		Sample											
		CS-S	CS-C	CS-N	SP-S	SP-C	SP-N	GB-S	GB-C	GB-N	GN-S	GN-C	GN-N
Sand minerals	Quartz	+	+	+	-	-	-	+	+	+	++++	++++	++++
	Feldspars / plagioclase	+	+	+	-	-	-	++	++	++	++	++	++
	chlorite	-	-	-	+	+	+	++	++	++	-	-	-
	mica	++++	++++	+++	-	-	-	+	+	+	++	++	++
	serpentine	+	+	++	++++	++++	++++	+	+	+	-	-	-
	amphiboles	-	-	-	-	-	-	++	++	++	-	-	-
Clay minerals	Quartz	+	+	+	-	-	-	+	+	+	+++	+++	+++
	Feldspars / plagioclase	+	+	+	-	-	-	+	+	+	+	+	+
	chlorite	-	-	+	-	-	-	+++	+++	+++	-	-	-
	Illite/mica	++++	++++	++++	-	-	-	+	+	+	++	++	++
	Hydroxi-interlayered minerals	-	-	-	-	-	-	-	-	-	+	+	+
	serpentine	++	++	+++	+++++	+++++	+++++	++	++	++	-	-	-
	amphiboles	-	-	-	-	-	-	+	+	+	-	-	-

687 Table 5: main chemical properties of the topsoil samples along the S-N transects crossing the

688 patterned ground features.

Site	Sample	Correspondence with genetic horizons*	pH	TOC	C/N	Exchangeable Ca	Exchangeable Mg	Exchangeable Ni	Available P
				%		cmol kg^{-1}	cmol kg^{-1}	mg kg^{-1}	mg kg^{-1}
CS	S	A	5.5	3.12	14.2	6.57	1.18	1.94	7.18
	SC	A (10%) - AC@ (30%) - CA@	5.3	3.01	14.3	3.76	1.23	3.50	2.66
	C	CA@ (10%) - C@1	6.0	1.12	18.7	1.15	0.31	6.94	1.35
	NC	AC@ (30%) - CA@	5.7	2.05	14.6	3.27	1.25	5.86	2.26
	N	A	5.2	2.65	14.7	6.32	2.05	11.77	8.09
	Cryptobiotic crust		5.3	8.73	19.0	6.42	1.99	8.38	14.32
SP	S	A(O)	5.4	11.78	13.4	5.02	4.57	30.24	10.77
	SC	A(O) (20%) AC@ (20%) - CA@ (30%) - C@ (30%)	5.9	3.33	15.1	1.31	1.97	20.12	2.26
	C	CA@ (40%) - C@1	6.1	1.21	13.4	0.88	0.99	16.36	1.25
	NC	AC@ (50%) - CA@	6.0	1.26	14.0	0.91	1.09	20.34	1.38
	N	A	5.7	1.59	13.3	1.30	1.64	24.74	2.41
GB	S	A	5.2	6.16	15.0	2.58	1.99	1.34	12.71
	SC	A(20%) - AC@(20%) - CA@	5.3	2.43	12.2	1.15	0.53	0.00	6.08
	C	CA@	6.4	0.42	10.5	1.02	1.05	1.57	0.68
	NC	A(60%) - CA@	5.6	0.95	13.6	0.97	1.44	0.18	2.04
	N	A	5.4	4.21	16.8	2.92	1.52	0.03	12.02
GN	S	Bw@	5.3	0.27	6.8	2.06	0.06	0.00	9.77
	SC	Bw@ (20%) - C@1	5.4	0.42	8.4	0.26	0.08	0.00	14.00
	C	Bw@	5.6	0.30	7.5	0.20	0.11	0.00	26.43
	NC	A (10%) - Bw@	5.4	0.52	8.7	0.22	0.08	0.00	16.46
	N	A	5.3	0.60	12.0	0.24	0.07	0.00	14.30

* the proportions of different horizons material has been calculated based on the depth trend of the surface horizons, as the top 10 cm were sampled during this phase of the work

692 Table 6: Plant species sampled in the observed patterned ground features.

	CS					SP					GB					GN				
	S	SC	C	NC	N	S	SC	C	NC	N	S	SC	C	NC	N	S	SC	C	NC	N
Thlaspietea rotundifolii (basic scree vegetation)																				
Cerastium pedunculatum								X						x						
Cerastium uniflorum															x	x				x
Saxifraga biflora				x																
Saxifraga bryoides						x	x	X	x	x	x	x		x	x					
Thlaspi rotundifolium subsp. *corymbosum*						x		X		x										
Salicetea herbaceae (humid snowbed)																				
Cardamine alpina																x	x			x
Carex foetida		x	x	x	x															
Carex parviflora							x													
Gentiana bavarica	x				x															
Gnaphalium supinum	x	x	x	x	x															
Leucanthemopsis alpina	x		x		x								x							
Luzula alpinopilosa		x					x			x										
Myosotis alpestris					x					x	x	x								
Pedicularis kerneri									x											
Poa laxa	x	x	x	x	x					x			x	x		x	x	x	x	x
Potentilla aurea	x	x			x															
Polygonum viviparum				x																
Salix herbacea		x	x	x	x						x	x			x					
Veronica bellidioides				x																
Caricetum curvulae (acidic alpine																				

grassland)															
Agrostis rupestris					x			x		x				x	X
Armeria alpina				x	x	X	x	x				x	x		
Carex curvula	x		x												
Euphrasia minima			x												
Festuca halleri		x		x					x		x			x	
Minuartia recurva										x	x		x		
Minuartia sedoides									x	x		x	x		
Phyteuma globulariifolium									x	x		x			
Sedum alpestre				x			x								X
Sempervivum montanum													x		
Silene acaulis							x		x			x	x	x	
Vaccinium uliginosum subsp. *gaultherioides*													x		
Other basophilous species															
Festuca quadriflora				x											
Saxifraga exarata subsp. *moschata*									x		x	x			
Serpentine endemics															
Carex fimbriata				x				x							

693

694

695 Table 7: correlation values and significance between the soil chemical properties and the NMDS

696 factors shown in Figure 5b

	NMDS1	NMDS2	r^2	p-value
Ni	0.99	0.17	0.32	0.04
P	-0.33	0.95	0.28	0.06
pH	0.91	0.41	0.04	0.71
Ca	-0.27	-0.96	0.26	0.07
Ca/Mg	-0.35	0.94	0.08	0.71
TOC	0.39	-0.72	0.17	0.19
C/N	0.17	-0.99	0.49	0.00
N	0.80	-0.60	0.14	0.27

697